

Review

Recent Advances in Selective Photo-Epoxidation of Propylene: A Review

Van-Huy Nguyen ^{1,2,*}, Ba-Son Nguyen ³, Hieu-Thao Vo ⁴, Chinh Chien Nguyen ⁵,
Sa-Rang Bae ⁶, Soo Young Kim ^{6,*} and Quyet Van Le ^{5,*}

¹ Department for Management of Science and Technology Development, Ton Duc Thang University, Ho Chi Minh City 700000, Vietnam

² Faculty of Applied Sciences, Ton Duc Thang University, Ho Chi Minh City 700000, Vietnam

³ Key Laboratory of Advanced Materials for Energy and Environmental Applications, Lac Hong University, Bien Hoa 810000, Vietnam; bason@lhu.edu.vn

⁴ HCMC University of Food Industry, Ho Chi Minh City 700000, Vietnam; vhiethao95@gmail.com

⁵ Institute of Research and Development, Duy Tan University, Da Nang 550000, Vietnam; nguyenchinhchien@duytan.edu.vn

⁶ Department of Materials Science and Engineering, Korea University 145, Anam-ro Seongbuk-gu, Seoul 02841, Korea; dngor1147@naver.com

* Correspondence: nguyenvanhuy@tdtu.edu.vn (V.-H.N.); sooyoungkim@korea.ac.kr (S.Y.K.); levanquyet@dtu.edu.vn (Q.V.L.)

Received: 16 December 2019; Accepted: 3 January 2020; Published: 7 January 2020



Abstract: The epoxidation of propylene to produce propylene oxide (PO) has a vital role in the industrial production of several commercial compounds and the synthesis of numerous intermediates, fine chemicals, and pharmaceuticals. However, the current PO production processes pose significant problems regarding the environment and economy. The direct photo-epoxidation of propylene using molecular oxygen (an ideal oxidant with active oxygen of 100 wt %) under light irradiation is a promising technology to produce PO. This process offers numerous advantages, including the use of simple technologies, low-cost methods, and environmental friendliness. Many efforts have focused on the design of new photocatalyst systems, optimizing the conditions for a photocatalytic reaction, and elucidating the mechanisms of photo-epoxidation. This review is expected to serve as a comprehensive background, providing researchers with insight into the recent developments regarding the direct photo-epoxidation of propylene.

Keywords: photo-epoxidation; propylene; photocatalyst; reaction conditions; mechanisms

1. Introduction

Among epoxides, propylene oxide (PO) is known to be an extremely reactive substance and an important chemical intermediate [1]. It is sometimes called 1,2-epoxypropane or 2-methyloxirane. This compound is widely used as the starting material to synthesize numerous commercial materials; these include polymers (polyurethanes and polyesters), oxygenated solvents (propylene glycol ethers), and industrial fluids (monopropylene glycol and polyglycols) [1]. Based on a market overview from Mordor Intelligence, PO is forecasted to gain at a compounded annual growth rate of approximately 5.9% during the forecast period of 2019–2024 [2].

Currently, the existing PO production processes are technologically divided into chlorohydrin, a coproduct (indirect oxidation or organic hydroperoxide), hydrogen peroxide, direct oxidation, and hydro oxidation processes [3]. A significant amount of PO is traditionally made using the chlorohydrin process, including chlor-alkali PO, lime PO, and PO (Lummu) routes, which suffer from environmental liabilities and have high capital costs. Alternative processes through indirect oxidation, including

Tert-butyl Alcohol (PO/TBA), styrene monomer propylene oxide (SMPO), and cumene hydroperoxide (CHP), have been commercialized. Since there is a long-term level of demand for their coproducts, it is expected that the organic hydroperoxide processes will maintain an essential role in propylene epoxidation. New PO technologies, namely hydrogen peroxide propylene oxide (HPPO) [4] and hydro oxidation [5], have recently been gaining in popularity. However, the low efficiency of hydrogen and safety considerations require hydrogen peroxide production facilities to apply such processes as only a temporary solution.

Among all alternative processes available, the direct photocatalytic propylene epoxidation process, using molecular oxygen as an oxidant, is the most feasible, because (1) molecular oxygen, which has active oxygen of 100 wt %, is an ideal oxidant; (2) solar light is a reliable, abundant, and green energy source; and (3) solar-driven photo-epoxidation can be easily performed at room temperature without a heat requirement. Although there are numerous advantages to photo-epoxidation, the practical applications for this approach are still challenges with many limitations, such as an inefficiency to exploit visible light, an unsatisfactory PO yield (low PO selectivity and inefficient propylene conversion), or the possible deactivation of a photocatalyst [6]. Therefore, although serious efforts have been made regarding the design of novel photocatalytic materials, the optimization of the reaction conditions required to meet these technical remains a challenge.

Of particular interest, this article highlights the important achievements in the designing of a photocatalyst [7–14] and the optimization of photo-epoxidation conditions, including the reaction temperature [15,16], light irradiation [17–19], and oxygen/propylene ratio [13,20]. In addition, the detailed mechanisms involved in the solar-driven epoxidation of propylene are systematically proposed. Finally, a perspective in this photo-epoxidation field is presented.

2. Designing Photocatalysts and the Role of Silica Supports

Many developed photocatalysts that function efficiently under UV and visible light have been successfully proposed for photo-epoxidation, and have remained a subject of significant interest [7–14,16,18,20–27]. Pichat et al. were the first to screen a series of oxides, such as TiO_2 , ZrO_2 , V_2O_5 , ZnO , SnO_2 , Sb_2O_4 , CeO_2 , WO_3 , and an Sn–O–Sb mixed oxide, for the photo-epoxidation of propylene at 320 K under UV-light [21]. Their results indicate that total oxidation predominates over CeO_2 , TiO_2 , ZrO_2 , and ZnO . In contrast, SnO_2 , WO_3 , and an Sn–O–Sb mixed oxide photo-catalyze only partial oxidation, whereas Sb_2O_4 yields a small percentage of CO_2 in addition to mild oxidation compounds. However, TiO_2 and ZrO_2 can produce PO with a selectivity of 10.5% and 5%, respectively. In addition, it was found that V_2O_5 is photo-inactive under experimental conditions. Surprisingly, V_2O_5 supported on SiO_2 efficiently promotes the partial photo-epoxidation of propylene into aldehydes [26,28]. Yoshida et al. systematically screened 50 types of silica-supported metal oxides for the photo-epoxidation of propylene (as shown in Figure 1) [10]. They found that silica modified with some candidate elements, such as Li, Na, Mg, Ca, Sr, Ba, Y, and La, could achieve a high selectivity to PO; however, their C_3H_6 conversions were quite low, and similar to those of the bulk silica. Silica loaded with some candidates, including Ti, Zn, Pb, and Bi can achieve high PO yields. Among the metal oxide supports, Ti and Zn are the most effective systems for the photo-epoxidation of propylene. Afterward, photocatalysts based on silica support have received considerable attention, owing to their photo-epoxidation. Some metal oxides supported by silica include Nb_2O_5 [25], MgO [20], ZnO_x [10], PbO_x [10], CrO_x [10,29,30], BiO_x [10], ZrO_x [10], V_2O_5 [14,29], and TiO_2 [9,10,12,29]. Silica-based photocatalysts have several advantages [31], including the following:

1. Extensive, highly dispersed, tetrahedrally coordinated metal oxides: some candidates, such as TiO_2 , V_2O_5 , Mo_2O_3 , and Cr_2O_3 moieties, could be successfully dispersed and isolated when implanting on the silica matrix. It has been noted that these dispersed and isolated Ti, V, Mo, and Cr transition metal oxides can be easily excited under light irradiation to construct corresponding

charge-transfer excited states that engage an electron dispatch from O^{2-} to M^{n+} , as shown in Equation (1).



This particular property concerns a single-site photocatalyst, which differs from a conventional photocatalyst [29,32]. The highly reactive and selective catalytic epoxidation of propylene under these charge-transfer excited states constructed, in which the states of electron-hole pairs are localized nearby on single-site heterogeneous catalysts, leads to such a significant photo-epoxidation.

2. Localization of the photoexcitation at the moiety because of the electric non-conductance of silica. Silica is a well-known electrical insulator, in theory. Thus, its photoexcitation (electron-hole pairs) is localized at the moiety of metal-oxygen and has a long lifetime, which favors photoexcitation.
3. Transparency support material: silica allows UV-visible light to pass through the material, and does not hamper significantly when the light reaches the photoactive sites.
4. Depression of side reaction: silica support is mostly inactive for a photocatalytic reaction.

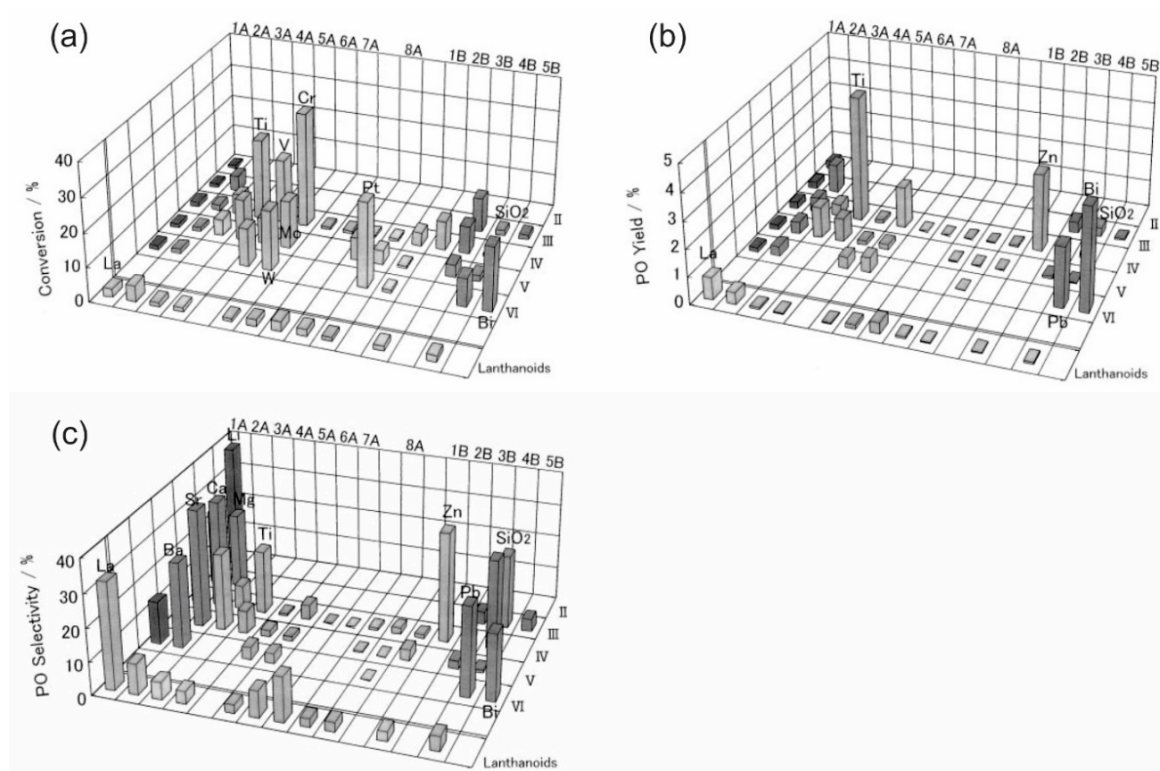


Figure 1. (a) Propylene conversion, (b) propylene oxide (PO) yield, and (c) PO selectivity over various silica-supported catalysts in the photo-epoxidation of propylene through molecular oxygen. The data is collected after 2 h in reaction. Reproduced with permission from [10].

Zeolites and mesoporous silica materials, such as titanium silicalite 1 (TS-1), mobile composition of matter (MCM) [33], Santa Barbara amorphous (SBA-15) [34], FSM-16 [35,36], and Technische Universiteit Delft (TUD-1) [37], are perfect hosts for the preparation of single-site photocatalysts, owing to their highly ordered and open structure. Among the above MCM materials, the structures of which are shown in Figure 2a–c, MCM-41 has received considerable attention [38]. Regarding the synthesis process of these composite materials, two approaches have used different structure-directing agents, including a true liquid-crystal and a cooperative liquid-crystal [38]. For the true liquid-crystal approach, the presence of precursor inorganic framework materials (normally tetraethyl (TEOS) or tetraethylorthosilicate (TMOS) is not required, since a lyotropic liquid-crystalline phase could be

formed at high concentration of the surfactant. On the other hand, it is also possible for this phase to form even at lower concentrations of surfactant molecules for the cooperative liquid–crystal approach.

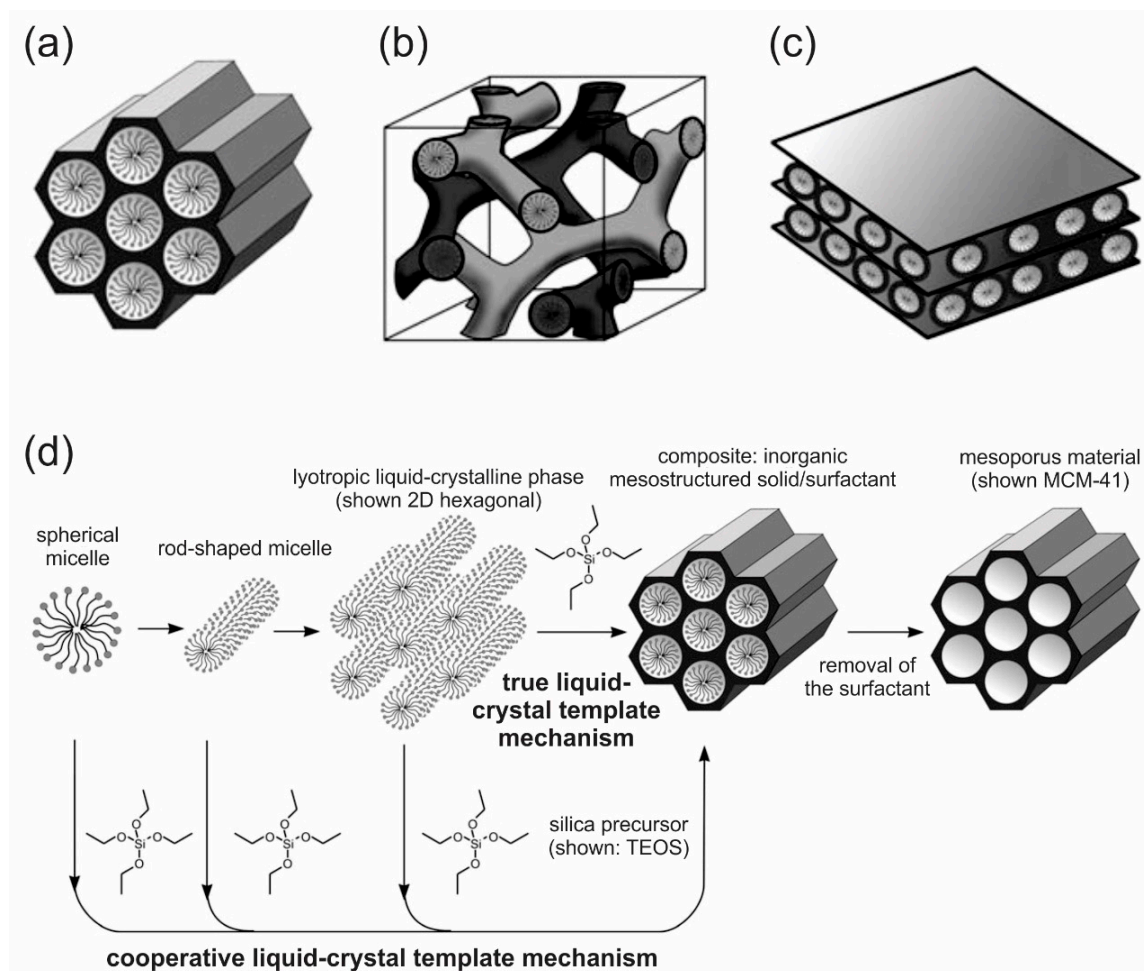


Figure 2. The different structures of mesoporous M41S materials: (a) mobile composition of matter (MCM)-41, (b) MCM-48, (c) MCM-50, and (d) the formation mechanism of mesoporous materials using structure-directing agents. Reproduced with permission from [38].

The most exciting feature properties of MCM-41 mesoporous material is its regular hexagonal array and hexagonally shaped pore (2–10 nm) structure, a high surface area (up to $1500 \text{ m}^2 \cdot \text{g}^{-1}$), and excellent thermal stability [39]. Nguyen et al. developed TS-1 and MCM-41 as matrixes to achieve single-site structure photocatalysts [7]. Interestingly, a notable synergistic photocatalytic performance over MCM-41 supporting binary V-/Ti-oxides was achieved during the photo-epoxidation of propylene [6]. Figure 3 clearly shows that two physically mixed photocatalysts ($\text{PxV}_{0.05}\text{Ti}_{0.2}$ and $\text{PxV}_{0.05}\text{Ti}_{0.6}$) achieved the catalytic performance within the range of the predicted activity. Hence, it is reasonable to conclude that a synergistic enhancement contributes to the significant difference between the predicted and observed performances. Among the candidates, $\text{V}_{0.05}\text{Ti}_{0.3}/\text{MCM-41}$ photocatalyst performed optimal synergistic photocatalytic activity on both PO formation and C_3H_6 consumption.

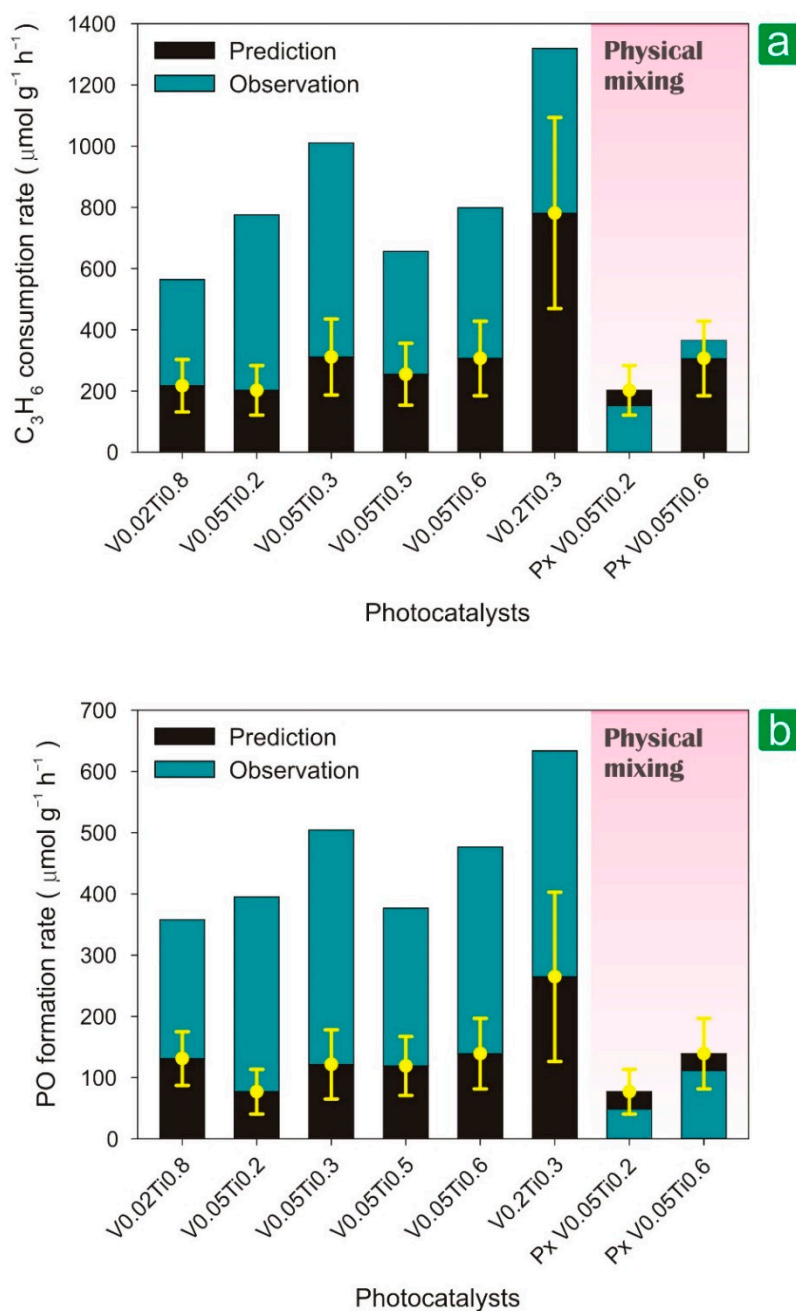


Figure 3. Contribution activity analysis for (a) C_3H_6 consumption and (b) PO formation rates. Reproduced with permission from [6].

A bismuth-based material, $\text{Bi}_2\text{WO}_6\text{-TiO}_2$, was recently developed, and has shown an excellent potential performance in photo-epoxidation [16]. Figure 4 clearly shows that two supporting materials with Bi_2WO_6 (BiWO-Ti50i and BiWO-Ti50i/GS) achieve better PO rates than a simple photocatalyst (Bi_2WO_6 , BW/GS , BW/Sil , and $\text{TiO}_2\text{-P25}$). However, PO selectivity is low, which becomes the greatest disadvantage of this catalyst system.

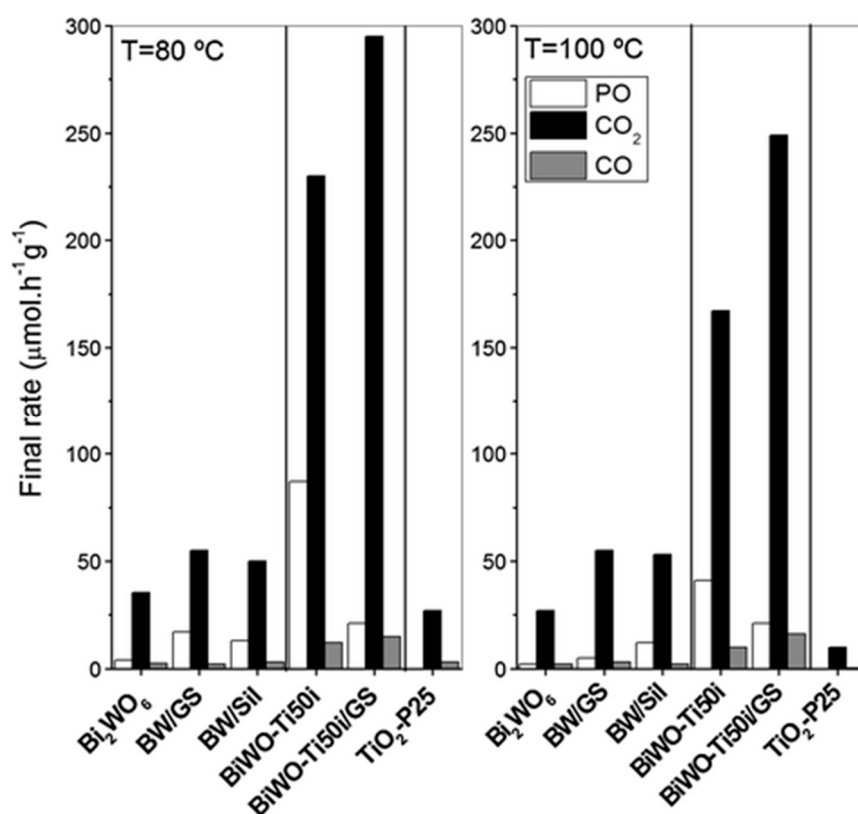


Figure 4. Formation rate of PO, CO₂, and CO obtained with different catalysts during photo-epoxidation at 80 °C and 100 °C. Reproduced with permission from [16].

3. Optimization of Experimental Conditions for Photo-Epoxidation

3.1. Effect of the Light Source

For the photo-epoxidation of propylene, the features of the light source (wavelength spectrum, types of light, light intensity, etc.) are crucial factors for efficient photocatalysis. Yamashita et al. used a high-pressure Hg lamp equipped with various UV cut-filters ($\lambda > 250$ nm, $\lambda > 340$ nm, $\lambda > 450$ nm) to conduct the photo-epoxidation experiment over mesoporous molecular sieve photocatalysts at 295 K [40]. The authors found that the reaction only proceeds on the V/Ti-HMS (hexagonal mesoporous silica) and Cr-HMS photocatalysts when using UV with $\lambda > 340$ nm, whereas no reaction occurs over the Ti-HMS photocatalyst. As the reason for this, V ions effectively shift the absorption band of Ti containing a mesoporous molecular sieve (Ti-HMS) toward longer wavelengths, whereas the chromium oxide moieties (Cr⁶⁺) dispersed in mesoporous silica are responsible for absorbing the long wavelength of visible light irradiation. In another approach, Nguyen et al. have successfully used artificial sunlight for the first time (a 300 W Xe lamp equipped with an AM1.5G filter) and UV light (a Hg Arc lamp equipped with various filters (365, 320–500, and 250–400 nm)) to drive the photo-epoxidation of propylene [19]. Since there is a limit on the light delivered to the photocatalyst that can be successfully absorbed, the authors proposed normalized light utilization (NLU) to indicate that the possible absorbed light could be consumed to activate the photoreaction.

$$\text{NLU} = \text{Intensity of light emitted} \times \text{Normalized absorption capability of photocatalyst} \quad (2)$$

As expected, the rate of PO formation and C₃H₆ consumption correlate with NLU in the log–log scale (as shown in Figure 5). This might conclude that photo-epoxidation over V-Ti/MCM-41 has a similar reaction mechanism under either UV light or UV–visible light/artificial sunlight.

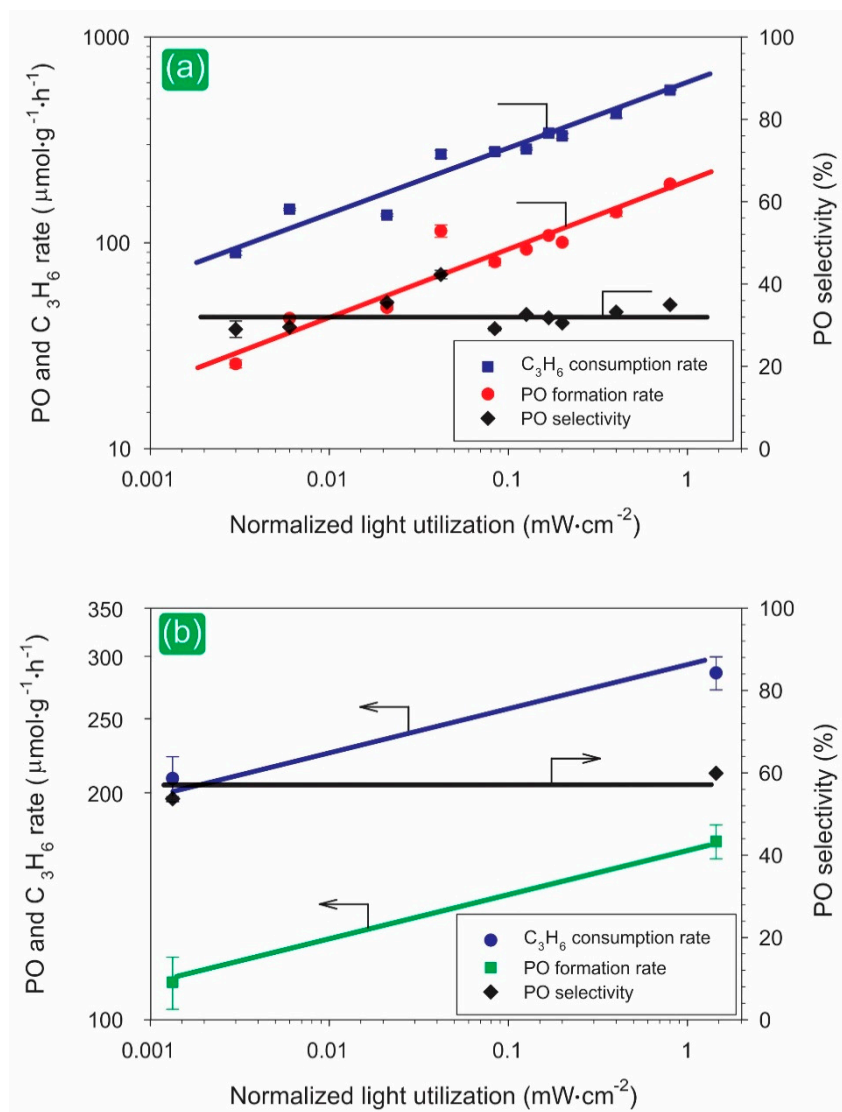


Figure 5. The correlation of catalytic activities versus normalized light utilization (NLU) over V-Ti/MCM-41: (a) a Hg Arc lamp and (b) a Xe lamp. Reproduced with permission from [19].

3.2. Effect of Reaction Temperature

In general, gas–solid heterogeneous reactions are significantly influenced by the reaction temperature; however, there is no obvious impact on a heterogeneous photocatalysis [41]. Very early on, Pichat et al. found that a rise in reaction temperature would harm the activity of photocatalytic epoxidation [21]. The results suggest that the temperature significantly influences the distribution in partial oxidation products. In a previous study, Nguyen et al. also found that the reaction temperature obviously alters the distribution of products in the photo-epoxidation of propylene [15]. Figure 6a shows that epoxidation selectivity firstly increases with the rise in temperature within the range of 298–323 K. Subsequently, a drop of selectivity toward PO is observed when the reaction temperature is maintained over 323 K. It should be noted that a rising reaction temperature favors the forming of PA (propionaldehyde), one of the most reactive aldehydes. This result is consistent with the finding by Yoshida et al., who reported that the reaction temperature influences the selectivity to the product and is favorable toward the formation of an aldehyde [28]. In another study, Li et al. also found that increasing the reaction temperature does not favor epoxidation selectivity [42]. The competition of multiple reactions toward different products might be attributed to this phenomenon. Therefore, the distribution of the products will be rearranged (as shown in Figure 6b).

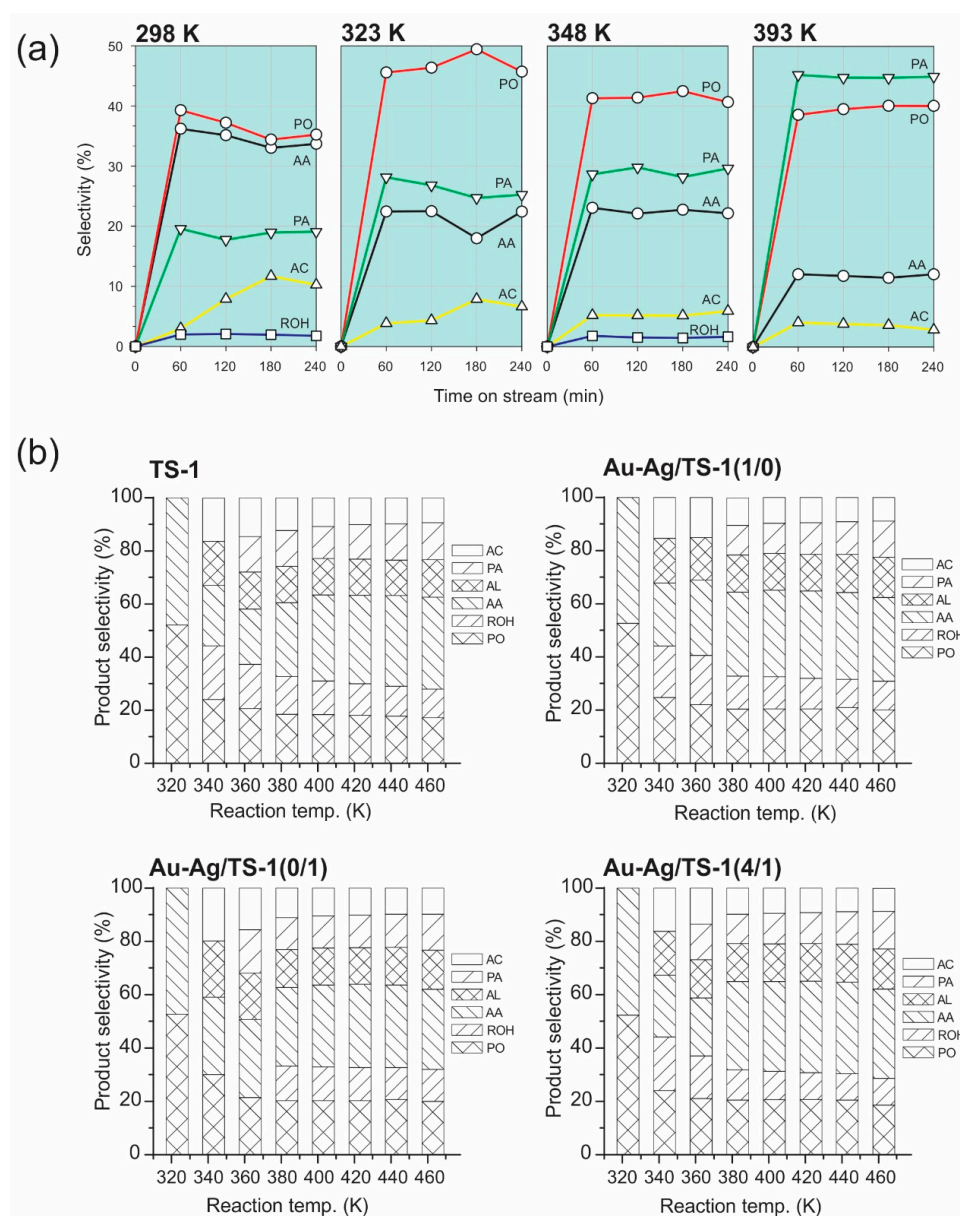


Figure 6. The selectivity to products for different temperature conditions: (a) V-Ti/MCM-41, reproduced with permission from [15]; and (b) Au-Ag/TS-1 photocatalysts, reproduced with permission from [42]. Abbreviations: propylene oxide (PO), propionaldehyde (PA), acetone (AC), acetaldehyde (AA), acrolein (AL), and ethanol (ROH).

In contrast, the reaction temperature also influences the conversion of propylene, by altering the adsorption of reactants and the desorption of products on the surface of photocatalyst. Generally, high temperatures tend to inhibit adsorption, because it is an exothermic process. Contrarily, increased temperature is beneficial to the desorption (endothermic process) and accelerates the surface reaction. As shown in Figure 7a, the reaction temperature has a dual action in terms of the reaction rate: (1) enhancing the desorption of products, which provides more active sites for the photocatalytic reaction; and (2) reducing the adsorption of reactants, which decreases the photocatalytic efficiency [15]. In another approach, Li et al. also observed the dual relationship between the reaction temperature (323–473 K) and the photocatalytic performance for the C_3H_6 conversion rate over an Au-Ag/TS-1 photocatalysts, as shown in Figure 7b [42].

In conclusion, the effect of reaction temperature on the photo-epoxidation of propylene is relatively complicated, with competing contributions. On the one hand, increasing the reaction temperature

can accelerate the surface reaction and favors the desorption of products (endothermic process) to release more active sites for a reaction, resulting in the promotion of a photocatalytic reaction. On the other hand, raising the reaction temperature might suppress the adsorption of reactants (exothermic process), which might inhibit the efficiency of the reaction.

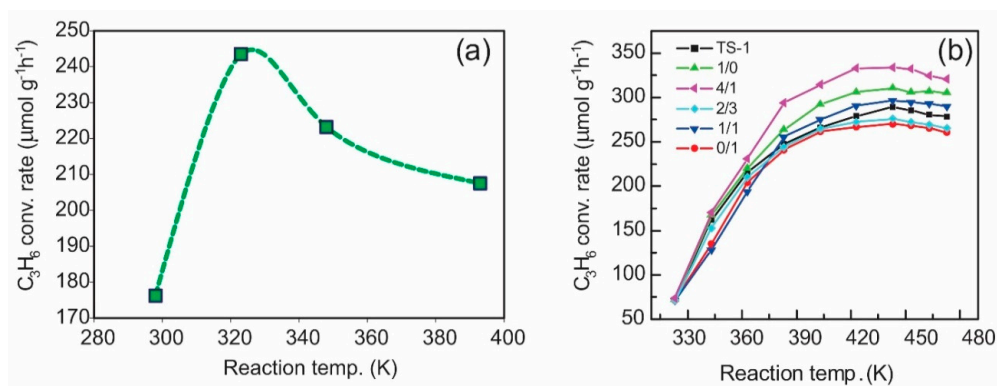


Figure 7. The influence of reaction temperature on the conversion rate of propylene: (a) V-Ti/MCM-41 [15] and (b) Au-Ag/TS-1 photocatalysts. Reproduced with permission from [42].

3.3. Effects of Oxygen/Propylene Ratio

Previous studies have also tested the effects of the different oxygen/propylene ratios on the photo-epoxidation system [13,20]. Figure 8 clearly illustrates the dependence on the different ratios of oxygen/propylene [13,20]. Obviously, a high oxygen/propylene ratio is favorable for the performance of photo-epoxidation. This result is highly consistent with an observation of direct epoxidation over silver catalysts [43,44]. Without the presence of oxygen, only a slight oxidation pathway towards acetaldehyde (AA) takes place over Mg-loaded silica. The photo-epoxidation of propylene towards PO in the presence of oxygen has been found. The optimal condition for achieving the best PO selectivity among the experiments studied was oxygen/propylene = 2. However, an excess amount of oxygen would push for the formation of other partial oxidation products.

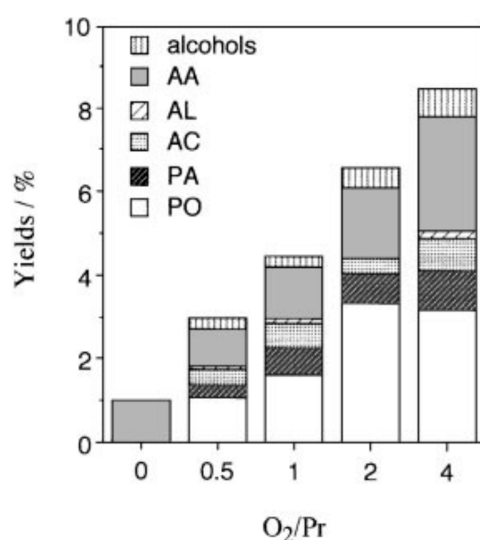


Figure 8. The influence of product yields on the oxygen/propylene ratio in the photo-epoxidation of propylene over Mg-loaded silica. Propylene: 30 μmol ; irradiation time of 2 h. Abbreviations: propylene oxide (PO), acetaldehyde (AA), propionaldehyde (PA), acetone (AC), acrolein (AL), and alcohols (methanol, ethanol, and propan-2-ol). Reproduced with permission from [20].

3.4. Effects of Co-Feeds

A further important parameter is the effect of co-feeds. This has been carefully investigated by Nguyen et al. in the photo-epoxidation of propylene over V-Ti/MCM-41 under UV-light irradiation of $0.3 \text{ mW}\cdot\text{cm}^{-2}$ at 323 K [27]. Figure 9 presents the correlation between H_2O vapor pressure and catalytic activity. It clearly shows that the photocatalytic activity is extremely influenced by the presence/absence of co-feeds; these include H_2O and H_2 . For H_2O , the photo-activity is quite complicated. And depends on the partial pressure of the co-feed. In the range of 0.0–0.6 kPa H_2O , the photocatalytic activity is increased with the increase of co-feed. On the other hand, the photocatalytic performance is not further promoted when the H_2O pressure is over 0.6 kPa. For H_2 (5.6 kPa), the presence of H_2 could promote both of photocatalytic activity and stability of photocatalyst. It should be noted that the mechanism of photo-epoxidation in the presence/absence of co-feeds might not be similar; therefore, an increase in both the AA selectivity and AA formation rate has been observed in the presence of co-feeds.

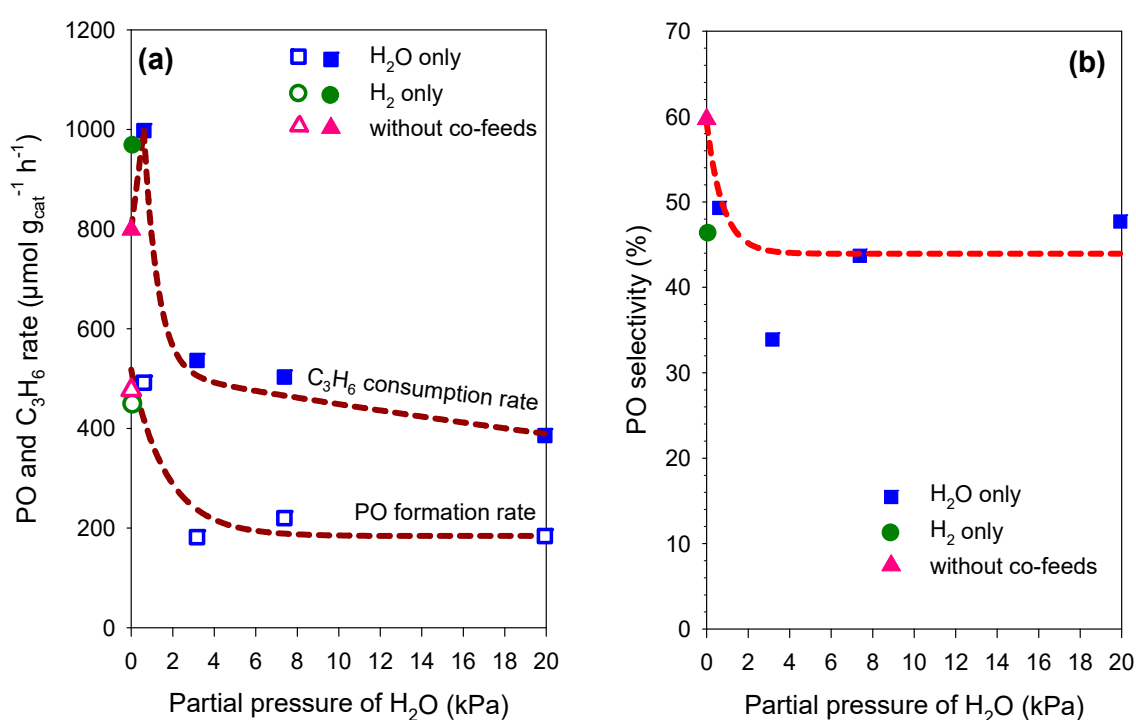


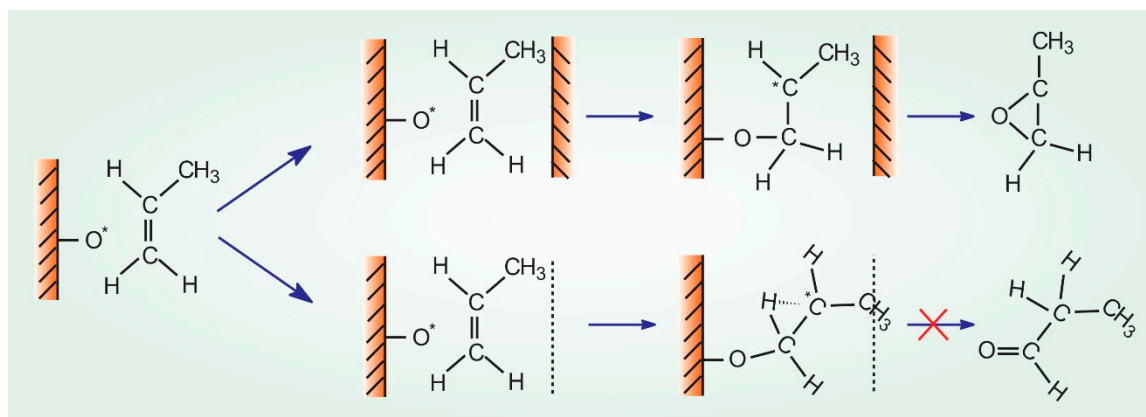
Figure 9. The influence of H_2O vapor pressures on (a) the C_3H_6 consumption rate and PO formation rate and (b) PO selectivity. Reproduced with permission from [27].

4. Elucidating Mechanisms of Photo-Epoxidation

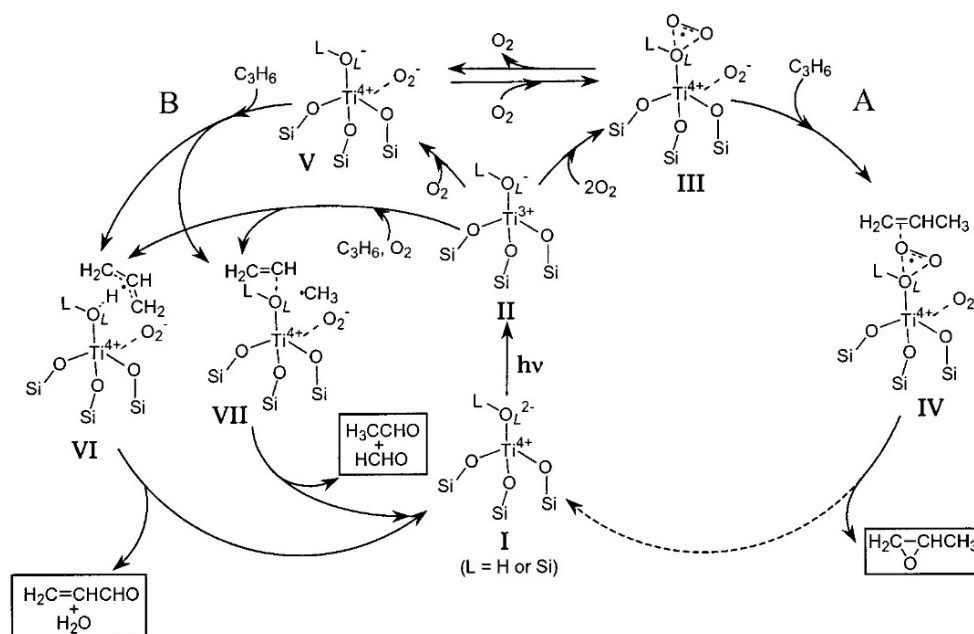
Since the intrinsic photocatalytic epoxidation mechanism is still not entirely clear, there is a strong effort to elucidate the reaction pathways of photo-epoxidation. In a previous study, Carter and Goddard suggested the reaction pathway to produce PO via an oxypropenyl intermediate through H-atom abstraction [45]. The critical role of the forming products is controlled by two factors: the reaction conditions and the angle of H-atom abstraction between attacking of the propylene and $\text{O}^*_{(\text{ads})}$. Based on H-atom abstraction, Nguyen et al. proposed possible reaction pathways to create PO and other intermediate species over an MCM-41-based photocatalyst (as seen in Scheme 1) [7]. They came up with the conclusion that the distribution of the products is affected by H-atom abstraction in a limited space, e.g., inside the pore. Under a restricted space, it would favor the selectivity to PO via the formation of the oxypropenyl intermediate.

Advances made in the mechanism were presented by Yoshida and co-workers [9], who successfully proposed that molecular oxygen is activated on the charge-transferred ($\text{Ti}^{3+}-\text{O}_L^-$)* radical pair, which is constructed under light irradiation (as illustrated in Scheme 2). First, the Ti^{3+} moiety will react with

O_2 to form O_2^- . However, O_2^- cannot activate propylene by itself. Then, the O_L^- moiety, which is known to be the center of the hole in lattice oxygen, will react with O_2 to form an O_3^- oxygen radical species, resulting in a reaction with propylene to yield PO. The authors proposed that O_3^- is an electrophilic oxygen species capable of the PO forming. When the O_L^- moiety reacts with propylene, there is a possible reaction pathway to produce acrolein (AL) and ethanal through H abstraction and C–C bond fission, respectively.



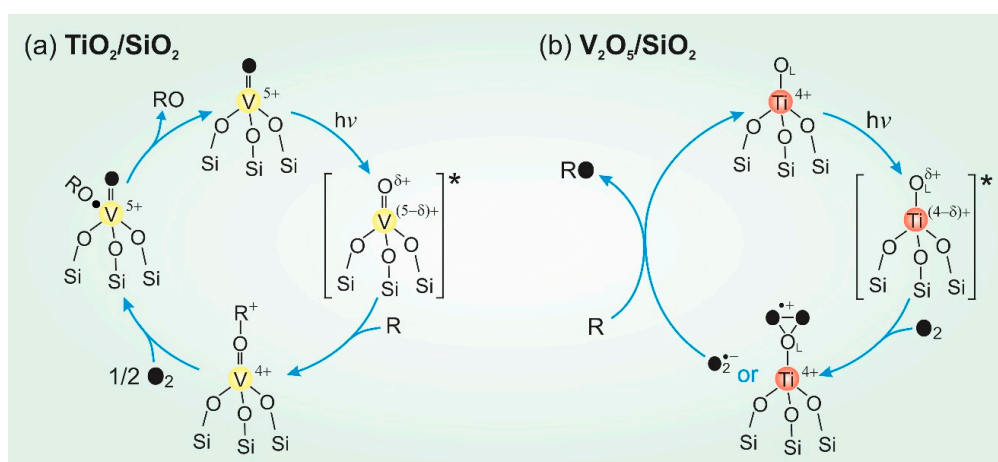
Scheme 1. The formation mechanism of PO and oxygenate products over V-Ti/MCM-41 photocatalysts. Reproduced with permission from [7].



Scheme 2. The proposed reaction mechanism in the photo-epoxidation of propylene over an isolated tetrahedral Ti species. Reproduced with permission from [9].

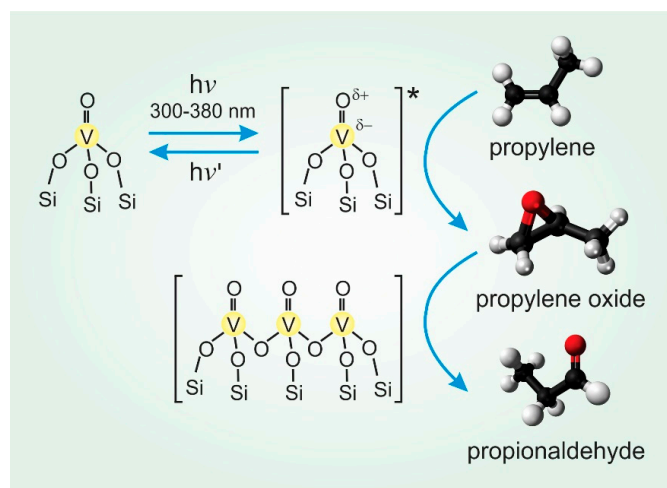
By contrast, Amano et al. suggested that both (O_2^-) and (O_3^-) oxygen radical species, which are created at the photo-formed hole center, can react with C_3H_6 over a Ti active site to generate PO and its co-products (as shown in Scheme 3a) [11]. For TiO_2/SiO_2 , the active oxygen species is derived directly from molecular oxygen to promote the photo-epoxidation. For V_2O_5/SiO_2 , the active oxygen species is formed by incorporating the O_L^- lattice oxygen of the surface metal oxide species. As expected, the active oxygen species (O_L^-) in the excited state of a ($V^{4+}-O_L^-$)* radical pair attacks the double bonds of C_3H_6 to generate a ($V^{4+}-O-C_3H_6^+$) species. Subsequently, the molecular oxygen takes the

photo-induced electron on the V cation to promote the selection to propylene epoxidation (as shown in Scheme 3b) [11].



Scheme 3. The proposed reaction mechanisms in the photo-epoxidation of propylene with molecular oxygen over (a) $\text{TiO}_2/\text{SiO}_2$ and (b) $\text{V}_2\text{O}_5/\text{SiO}_2$ [11].

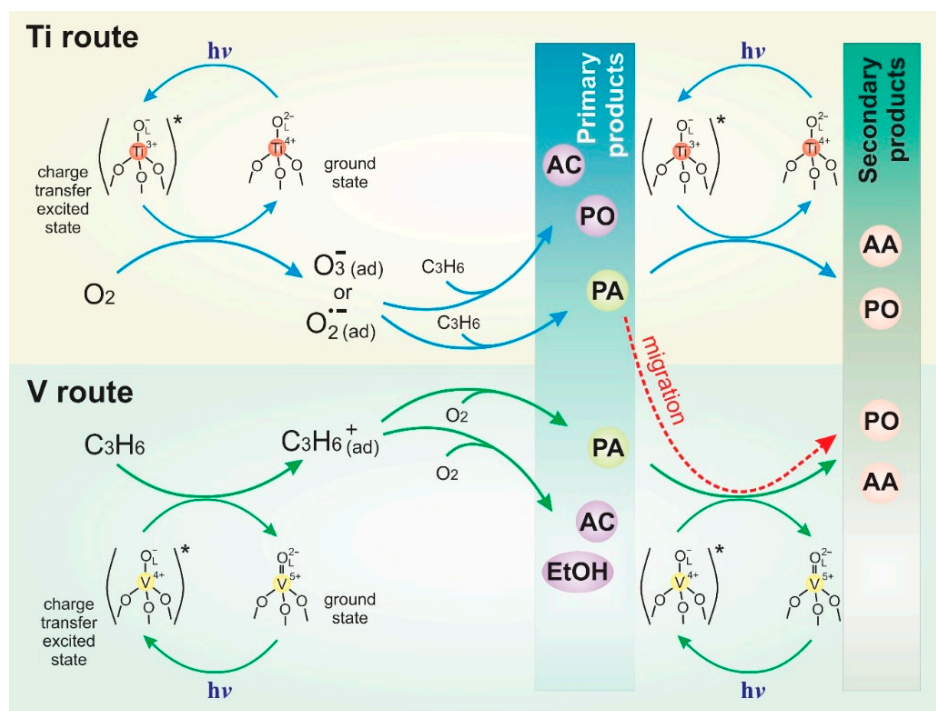
In another approach, Amano et al. proposed the impact of dispersed V^{5+} species on the distribution of products [46]. They found that $\text{V}_2\text{O}_5/\text{SiO}_2$, which contains less dispersed V^{5+} species, would promote the forming of PA. In detail, Scheme 4 depicts the mechanism of the photo-epoxidation of propylene with molecular oxygen over $\text{V}_2\text{O}_5/\text{SiO}_2$ [46]. The photo-excited $(\text{V}=\text{O})^*$ species of monomeric VO_4 tetrahedral dispersed in SiO_2 are photocatalytic active sites in the formation of PO, whereas the lowly dispersed vanadium oxide species in SiO_2 promotes the formation of PA via the isomerization of PO.



Scheme 4. The proposed reaction mechanism in propylene photo-epoxidation with molecular oxygen over $\text{V}_2\text{O}_5/\text{SiO}_2$ [46].

As mentioned above, both V and Ti metal oxide play an essential role in the photo-epoxidation of propylene. However, there has been a notable lack of answers regarding how V and Ti metal oxide promote the forming of PO. In their previous study, Nguyen et al. proposed a possible reaction mechanism in the photo-epoxidation of propylene on V- and Ti-oxide-modified MCM-41 photocatalysts (as shown in Scheme 5) [6]. Clearly, either V- or Ti-oxide could individually photo-epoxidize propylene under light irradiation. They found that the primary products of Ti-oxides are AC, PO, and PA, whereas those of V-oxides are AC, EtOH, and PA. It should be noted that Ti-oxide could generate PO directly from propylene, resulting in a higher achieved PO selectivity compared with V-oxides.

Based on the possible traveling species, two possible reaction pathways of the synergetic photo-activity could be proposed in the binary V-/Ti-oxides. First, the direct photo-epoxidation to produce PO, which is promoted by the Ti-oxides, is still preserved in the binary V-/Ti-oxides. Second, the indirect photo-epoxidation to produce PO is further enhanced by the possible traveling of PA. The PA traveling, which is produced on the Ti-sites, might travel to the V-sites and be photo-transformed on the V-sites. The V-sites, as compared with the Ti-sites, have a higher possibility to produce the PO through an indirect pathway. Hence, when PA traveling is photo-transformed in the V-sites, the photo-epoxidation is dramatically promoted.



Scheme 5. The proposed synergetic reaction mechanism in photo-epoxidation of propylene over V-Ti/MCM-41. Reproduced with permission from [6].

5. Comparison of the Photo-Epoxidation Process and Others

Although the experimental conditions required for photo-epoxidation of propylene differ, it is worth comparing their performance in terms of the selectivity and product yield (as shown in Figure 10). Amano et al. proposed V_2O_5/SiO_2 photocatalyst as an optimal candidate in their group [11]. By modifying the photo-excited lattice oxygen of V_2O_5/SiO_2 through an alkali, Amano et al. observed a high PO yield of $10.1 \text{ g}\cdot\text{kg}_{\text{cat}}^{-1}\cdot\text{h}^{-1}$ [14]. In another approach, BiWO₃-Ti50i/GS performed an optimal performance, with a PO yield of $16.9 \text{ g}\cdot\text{kg}_{\text{cat}}^{-1}\cdot\text{h}^{-1}$ [16]. In a recent study, Nguyen et al. proposed a V-Ti/MCM-41 in which its PO yield was boosted more than two-fold compared with BiWO₃-Ti50i/GS [6].

To further understand the current status of performance over different propylene epoxidation processes, a broad comparison based on the selectivity and turnover frequency (TOF) was successfully collected and evaluated (Figure 11). As mentioned earlier, HPPO is a primary green technology currently used in the production of industrial compounds. For the two HPPOs of the commercial Halcon styrene monomer and Degussa-Huls-Headwaters hydrogen peroxide process, their TOFs could reach up to 0.11 s^{-1} and $2.2 \times 10^{-2} \text{ s}^{-1}$, respectively [47]. It should be noted that the required TOF for industrial-scale production is approximately 0.1 s^{-1} . Gold deposited catalysts have recently received considerable attention for propylene epoxidation via hydro oxidation with the presence of O_2 and H_2 mixtures. Among potential candidates [48–50], a 0.05 Au/TS-1(36) catalyst provided a high TOF of 0.33 s^{-1} . For homogeneous systems, TOF was found to be within the range of 5.7×10^{-3} to

$2.0 \times 10^{-2} \text{ s}^{-1}$ [47,51]. The aforementioned catalytic processes afford an attractive TOF and selectivity; however, the requirement of either H_2O_2 or H_2 as the oxidant raises economic and safety concerns. The biological process performs an excellent TOF (12 s^{-1}) [52]. However, this process also raises some challenges, including the need for life-support systems, the product toxicity for microorganisms, the supply of cofactors, and the stability of the enzymes. To solve the above issues, direct photo-epoxidation with molecular oxygen was successfully proposed. However, the current result still remains far from the required TOF for large-scale production ($\text{TOF} = 0.1 \text{ s}^{-1}$). For more details, Table 1 summarizes all of the above reaction conditions and their performance with regard to propylene epoxidation.

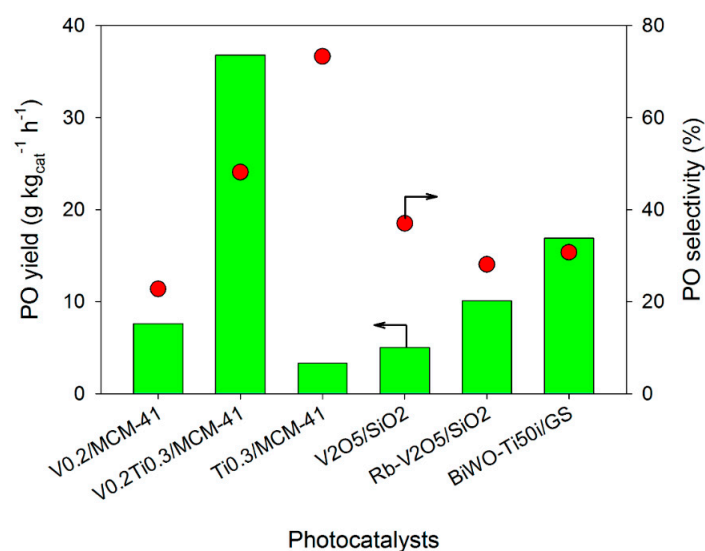


Figure 10. The comparison of PO yield and selectivity to PO for different photocatalyst systems.

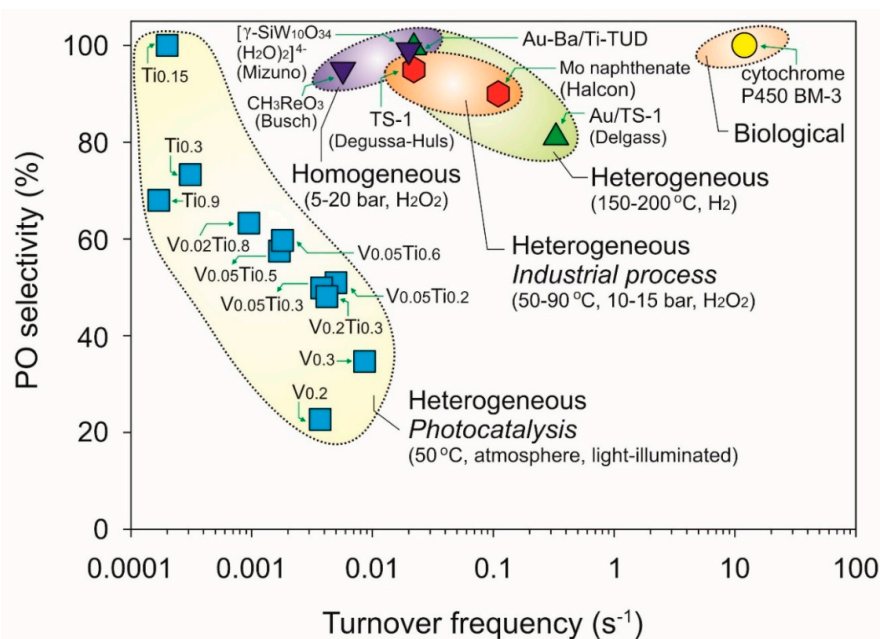


Figure 11. The correlation of turnover frequency versus selectivity for different propylene epoxidation processes. Reproduced with permission from [6].

Table 1. Epoxidation of propylene reactions and their catalysts.

No.	Type of Reactions	Catalysts	Reaction Conditions						Epoxidation Performances				Ref.
			Dosage (g _{cat})	Light	Temp. (°C)	Feeds	GHSV (mL·g _{cat} ⁻¹ ·h ⁻¹)	Others	Conv. (%)	Select. (%)	Yield (g·kg _{cat} ⁻¹ ·h ⁻¹)	TOF (s ⁻¹)	
1	Heterogeneous Photocatalysis	V _{0.2} /MCM-41	0.01	UV-light: 0.3 mW·cm ⁻²	50	C ₃ H ₆ /O ₂ /N ₂ = 1/1/16	360,000	N/A	0.07	22.7	7.6	3.70 × 10 ⁻³	[6]
2		V _{0.2} Ti _{0.3} /MCM-41							0.16	48.1	36.8	4.20 × 10 ⁻³	
3		Ti _{0.3} /MCM-41							0.01	73.3	3.3	0.30 × 10 ⁻³	
4		0.1 mol % V ₂ O ₅ /SiO ₂	0.3	300 W Xe arc lamp	30	C ₃ H ₆ /O ₂ /He = 2:1:7	20,000	N/A	N/A	37.0	5.0	N/A	[11]
5		Rb ion-modified 0.5 wt % V ₂ O ₅ /SiO ₂	0.3	300 W Xe arc lamp	50	C ₃ H ₆ /O ₂ /He = 2:1:7	5000	N/A	1.56	28.1	10.1	N/A	[14]
6		BiWO ₃ -Ti ₅₀ i/GS	20	UV-LEDs: 90 mW·cm ⁻²	80	N/A	1500	N/A	N/A	30.7	16.9	N/A	[16]
7		Au-Ag/TS-1 (4/1)	0.1	100 W high-pressure Hg lamp: 90 mW·cm ⁻²	N/A	N/A	12,720	N/A	N/A	52.3	3.97	N/A	[42]
8	Heterogeneous Halcon styrene monomer process	Mo naphthenate + K naphthenate promoter	N/A	N/A	90	N/A	N/A	EBHP; 10 bar	92.00 (H ₂ O ₂ conv.)	90.0	72	0.11	[47]
9	Heterogeneous Degussa-Huls-Headwaters hydrogen peroxide process	TS-1 + liquid base promoter (ammonia)	N/A	N/A	50	H ₂ O ₂ with H ₂ O solvent, MeOH, and MTBE	N/A	15 bar, pH = 8.5	19.00	95.0	770	2.20 × 10 ⁻²	[47]
10	Heterogeneous Hydrogen process	0.05 Au/TS-1(36)	0.3	N/A	200	C ₃ H ₆ /H ₂ /O ₂ /He = 1/1/1/7	7000	N/A	8.80	81.0	116	0.33	[48]
11		Au-Ba/Ti-TUD	N/A	N/A	150	C ₃ H ₆ /H ₂ /O ₂ /He = 1/1/1/7	7000	N/A	1.40	99.6	25	2.20 × 10 ⁻²	[49]
12		Au-TiO ₂ (0.05)@SBA-15	0.1	N/A	80	C ₃ H ₆ /H ₂ /O ₂ /He = 1/1/1/7	15,000	N/A	2.30 (H ₂ conv.)	62.0	51.8	N/A	[50]
			0.1	N/A	150	C ₃ H ₆ /H ₂ /O ₂ /He = 1/1/1/7	15,000	N/A	19.00	99.0	17.1	N/A	
13	Homogeneous Busch system	CH ₃ ReO ₃ , pyridine-N-oxide	N/A	N/A	30	H ₂ O ₂ with CH ₃ OH solvent	N/A	20 bar N ₂	N/A	>95.0	N/A	5.70 × 10 ⁻³	[47]
14	Homogeneous Mizuno system, closed system	tetra- <i>n</i> -butylammonium salt [γ-SiW ₁₀ O ₃₄ (H ₂ O) ₂] ⁴⁻	8 μmol	N/A	32	Propylene (6 atm, 5 mmol); 30% aq. H ₂ O ₂ (1 mmol), acetonitrile (6 mL)	N/A	8 h	99.00 (H ₂ O ₂ conv.)	>99.0	Yield of 90%	2.00 × 10 ⁻²	[47,51]
15	Biological	cytochrome P450 BM-3 139-3	N/A	N/A	25	N/A	N/A	1 atm, pH 8, NADPH	N/A	100.0	N/A	12.00	[52]

GHSV: gas hourly space velocity; TOF: turnover frequency; N/A: not available; Temp.: temperature; Conv.: conversion; Select.: selectivity; TUD: Technische Universiteit Delft.

6. Summary and Future Perspectives

This review is expected to serve as comprehensive background knowledge and to provide researchers with insight into the recent developments of the direct photo-epoxidation of propylene. This process using molecular oxygen (ideal oxidant with 100 wt % of active oxygen), which utilizes light energy in an active reaction, as a promising technology used to produce PO, owing to its potentially clean, low-cost, and straightforward advantages. Numerous efforts have focused on the design of new photocatalyst systems for optimizing the photocatalytic reaction conditions and elucidating the mechanisms of photo-epoxidation. Although significant improvements in photo-efficiency have been obtained for photocatalytic epoxidation, the results are still far from the required TOF for industrial-scale production ($\text{TOF} = 0.1 \text{ s}^{-1}$). Therefore, a goal in the coming years will be the continual development of new and effective photocatalyst systems. To promote the feasibility of and open up new opportunities for the photo-epoxidation of propylene, the following criteria should be directly addressed:

- The mechanisms and kinetics of the photo-epoxidation of propylene should be elucidated and determined at a fundamental level. Understanding their roles can support the design of effective photocatalysts in the future.
- Novel photocatalysts should be tailored that can widen visible light absorption, strengthen the forward reaction, depress the reverse reaction, achieve a recombination of photogenerated electron–hole pairs, prolong the lifetime of photogenerated electron–hole pairs, and favor the adsorption of reactants, with a particular focus on the metal oxides supported on zeolites and mesoporous silica photocatalytic materials.
- Novel photocatalytic systems, including photoreactors and reaction conditions that can upgrade the mass transfer, photon transfer, distribution, and usage of the light source should be designed and prepared for a scale-up through a reconstruction of the current systems.

Funding: This research was supported in part by the Bio and Medical Technology Development Program (2018M3A9H1023141) of the National Research Foundation of Korea (NRF), funded by the Korean government, and in part by the Korea Agency for Infrastructure Technology Advancement grant (17IFIP-B133622-01), funded by the Ministry of Land and Infrastructure.

Conflicts of Interest: The authors declare no conflict of interest.

Abbreviations

PO: propylene oxide; PA: propionaldehyde; AC: acetone; AA: acetaldehyde, AL: acrolein; ROH: ethanol; TOF: turnover frequency; Tert-butyl Alcohol: PO/TBA; styrene monomer propylene oxide: SMPO; cumene hydroperoxide: CHP; hydrogen peroxide propylene oxide: HPPO; titanium silicalite 1: TS-; Technische Universiteit Delft: TUD-1; mobile composition of matter: MCM; Santa Barbara Amorphous: SBA-15.

References

1. Baer, H.; Bergamo, M.; Forlin, A.; Pottenger, L.H.; Lindner, J. Propylene oxide. In *Ullmann's Encyclopedia of Industrial Chemistry*; MCB UP Ltd.: Bingley, UK, 2012. [CrossRef]
2. Propylene Oxide Market—Growth, Trends, and Forecast (2019–2024). Available online: <https://www.mordorintelligence.com/industry-reports/propylene-oxide-market> (accessed on 5 October 2019).
3. Tsuji, J.; Yamamoto, J.; Ishino, M.; Oku, N. Development of new propylene oxide process. *Sumitomo Kagaku* **2006**, *1*, 4–10.
4. Russo, V.; Tesser, R.; Santacesaria, E.; Di Serio, M. Chemical and technical aspects of propene oxide production via hydrogen peroxide (HPPO process). *Ind. Eng. Chem. Res.* **2013**, *52*, 1168–1178. [CrossRef]
5. Kuperman, A.; Bowman, R.G.; Clark, H.W.; Hartwell, G.E.; Schoeman, B.J.; Tuinstra, H.E.; Meima, G.R. Process for the Hydro-Oxidation of Olefins to Olefin Oxides Using Oxidized old Catalyst. Google Patents US6255499B1, 3 July 2001.
6. Nguyen, V.-H.; Lin, S.D.; Wu, J.C.-S. Synergetic photo-epoxidation of propylene over VTi/MCM-41 mesoporous photocatalysts. *J. Catal.* **2015**, *331*, 217–227. [CrossRef]

7. Nguyen, V.-H.; Chan, H.-Y.; Wu, J.C.S.; Bai, H. Direct gas-phase photocatalytic epoxidation of propylene with molecular oxygen by photocatalysts. *Chem. Eng. J.* **2012**, *179*, 285–294. [[CrossRef](#)]
8. Nguyen, V.-H.; Chan, H.-Y.; Wu, J. Synthesis, characterization and photo-epoxidation performance of Au-loaded photocatalysts. *J. Chem. Sci.* **2013**, 1–9. [[CrossRef](#)]
9. Murata, C.; Yoshida, H.; Kumagai, J.; Hattori, T. Active sites and active oxygen species for photocatalytic epoxidation of propene by molecular oxygen over TiO₂–SiO₂ binary oxides. *J. Phys. Chem. B* **2003**, *107*, 4364–4373. [[CrossRef](#)]
10. Yoshida, H.; Murata, C.; Hattori, T. Screening study of silica-supported catalysts for photoepoxidation of propene by molecular oxygen. *J. Catal.* **2000**, *194*, 364–372. [[CrossRef](#)]
11. Amano, F.; Yamaguchi, T.; Tanaka, T. Photocatalytic oxidation of propylene with molecular oxygen over highly dispersed titanium, vanadium, and chromium oxides on silica. *J. Phys. Chem. B* **2005**, *110*, 281–288. [[CrossRef](#)]
12. Yoshida, H.; Murata, C.; Hattori, T. Photocatalytic epoxidation of propene by molecular oxygen over highly dispersed titanium oxide species on silica. *Chem. Commun.* **1999**, 1551–1552. [[CrossRef](#)]
13. Yoshida, H.; Tanaka, T.; Yamamoto, M.; Funabiki, T.; Yoshida, S. Photooxidation of propene by O₂ over silica and Mg-loaded silica. *Chem. Commun.* **1996**, 2125–2126. [[CrossRef](#)]
14. Amano, F.; Tanaka, T. Modification of photocatalytic center for photo-epoxidation of propylene by rubidium ion addition to V₂O₅/SiO₂. *Catal. Commun.* **2005**, *6*, 269–273. [[CrossRef](#)]
15. Nguyen, V.-H.; Wu, J.C.S.; Bai, H. Temperature effect on the photo-epoxidation of propylene over V–Ti/MCM-41 photocatalyst. *Catal. Commun.* **2013**, *33*, 57–60. [[CrossRef](#)]
16. Murcia-López, S.; Vaiano, V.; Sannino, D.; Hidalgo, M.C.; Navío, J.A. Photocatalytic propylene epoxidation on Bi₂WO₆-based photocatalysts. *Res. Chem. Intermediat.* **2014**, 1–14. [[CrossRef](#)]
17. Wong, J.; Lytle, F.W.; Messmer, R.P.; Maylotte, D.H. K-edge absorption spectra of selected vanadium compounds. *Phys. Rev. B* **1984**, *30*, 5596–5610. [[CrossRef](#)]
18. Nguyen, V.-H.; Chan, H.-Y.; Wu, J.C.S.; Bai, H. Photo-epoxidation of propylene to propylene oxide over V-Ti/MCM-41: A wavelength effect on photocatalytic activities. In Proceedings of the 14th Asia Pacific Confederation of Chemical Engineering Congress, Singapore, 22–24 February 2012.
19. Nguyen, V.-H.; Lin, S.D.; Wu, J.C.-S.; Bai, H. Artificial sunlight and ultraviolet light induced photo-epoxidation of propylene over V-Ti/MCM-41 photocatalyst. *Beilstein J. Nanotechnol.* **2014**, *5*, 566–576. [[CrossRef](#)] [[PubMed](#)]
20. Yoshida, H.; Tanaka, T.; Yamamoto, M.; Yoshida, T.; Funabiki, T.; Yoshida, S. Epoxidation of propene by gaseous oxygen over silica and Mg-Loaded silica under photoirradiation. *J. Catal.* **1997**, *171*, 351–357. [[CrossRef](#)]
21. Pichat, P.; Herrmann, J.M.; Disdier, J.; Mozzanega, M.N. Photocatalytic oxidation of propene over various oxides at 320 K. Selectivity. *J. Phys. Chem.* **1979**, *83*, 3122–3126. [[CrossRef](#)]
22. Xiang, Y.; Larsen, S.C.; Grassian, V.H. Photooxidation of 1-Alkenes in zeolites: A study of the factors that influence product selectivity and formation. *J. Am. Chem. Soc.* **1999**, *121*, 5063–5072. [[CrossRef](#)]
23. Blatter, F.; Sun, H.; Vasenkov, S.; Frei, H. Photocatalyzed oxidation in zeolite cages. *Catal. Today* **1998**, *41*, 297–309. [[CrossRef](#)]
24. Blatter, F.; Sun, H.; Frei, H. Selective oxidation of propylene by O₂ with visible light in a zeolite. *Catal. Lett.* **1995**, *35*, 1–12. [[CrossRef](#)]
25. Tanaka, T.; Nojima, H.; Yoshida, H.; Nakagawa, H.; Funabiki, T.; Yoshida, S. Preparation of highly dispersed niobium oxide on silica by equilibrium adsorption method. *Catal. Today* **1993**, *16*, 297–307. [[CrossRef](#)]
26. Yoshida, S.; Magatani, Y.; Noda, S.; Funabiki, T. Partial oxidation of propene over U.V.-irradiated vanadium oxide supported on silica. *J. Chem. Soc. Chem. Commun.* **1981**, 601–602. [[CrossRef](#)]
27. Nguyen, V.-H.; Lin, S.D.; Wu, J.C.S.; Bai, H. Influence of co-feeds additive on the photo-epoxidation of propylene over V–Ti/MCM-41 photocatalyst. *Catal. Today* **2015**, *245*, 186–191. [[CrossRef](#)]
28. Yoshida, S.; Tanaka, T.; Okada, M.; Funabiki, T. Mechanism of photo-oxidation of propene over vanadium oxide supported on silica. *J. Chem. Soc. Faraday Trans.* **1984**, *80*, 119–128. [[CrossRef](#)]
29. Anpo, M.; Kim, T.-H.; Matsuoka, M. The design of Ti-, V-, Cr-oxide single-site catalysts within zeolite frameworks and their photocatalytic reactivity for the decomposition of undesirable molecules—The role of their excited states and reaction mechanisms. *Catal. Today* **2009**, *142*, 114–124. [[CrossRef](#)]
30. Murata, C.; Yoshida, H.; Hattori, T. Visible light-induced photoepoxidation of propene by molecular oxygen over chromia-silica catalysts. *Chem. Commun.* **2001**, 2412–2413. [[CrossRef](#)]

31. Yoshida, H. Active sites of silica-based quantum photocatalysts for non-oxidative reactions. *Catal. Surv. Asia* **2005**, *9*, 1–9. [[CrossRef](#)]
32. Anpo, M.; Thomas, J.M. Single-site photocatalytic solids for the decomposition of undesirable molecules. *Chem. Commun.* **2006**, 3273–3278. [[CrossRef](#)]
33. Kresge, C.T.; Leonowicz, M.E.; Roth, W.J.; Vartuli, J.C.; Beck, J.S. Ordered mesoporous molecular sieves synthesized by a liquid-crystal template mechanism. *Nature* **1992**, *359*, 710–712. [[CrossRef](#)]
34. Zhao, D.; Feng, J.; Huo, Q.; Melosh, N.; Fredrickson, G.H.; Chmelka, B.F.; Stucky, G.D. Triblock copolymer syntheses of mesoporous silica with periodic 50 to 300 angstrom pores. *Science* **1998**, *279*, 548–552. [[CrossRef](#)]
35. Inagaki, S.; Fukushima, Y.; Kuroda, K. Synthesis of highly ordered mesoporous materials from a layered polysilicate. *J. Chem. Soc. Chem. Commun.* **1993**, 680–682. [[CrossRef](#)]
36. Ishikawa, T.; Matsuda, M.; Yasukawa, A.; Kandori, K.; Inagaki, S.; Fukushima, T.; Kondo, S. Surface silanol groups of mesoporous silica FSM-16. *J. Chem. Soc. Faraday Trans.* **1996**, *92*, 1985–1989. [[CrossRef](#)]
37. Jansen, J.C.; Shan, Z.; Marchese, L.; Zhou, W.; Puil, N.v.d.; Maschmeyer, T. A new templating method for three-dimensional mesopore networks. *Chem. Commun.* **2001**, 713–714. [[CrossRef](#)]
38. Hoffmann, F.; Cornelius, M.; Morell, J.; Fröba, M. Silica-based mesoporous organic–inorganic hybrid materials. *Angew. Chem. Int. Ed.* **2006**, *45*, 3216–3251. [[CrossRef](#)]
39. Grün, M.; Unger, K.K.; Matsumoto, A.; Tsutsumi, K. Novel pathways for the preparation of mesoporous MCM-41 materials: control of porosity and morphology. *Microporous Mesoporous Mater.* **1999**, *27*, 207–216. [[CrossRef](#)]
40. Yamashita, H.; Kida, K.; Ikeue, K.; Kanazawa, Y.; Yoshizawa, K.; Anpo, M. Photocatalytic epoxidation of propene with molecular oxygen under visible light irradiation on V ion-implanted Ti-HMS and Cr-HMS mesoporous molecular sieves. In *Studies in Surface Science and Catalysis*; Park, S.-E., Ryoo, R., Ahn, W.-S., Lee, C.W., Chang, J.-S., Eds.; Elsevier: Amsterdam, The Netherlands, 2003; Volume 146, pp. 597–600.
41. Fox, M.A.; Dulay, M.T. Heterogeneous photocatalysis. *Chem. Rev.* **1993**, *93*, 341–357. [[CrossRef](#)]
42. Li, N.; Yang, B.; Liu, M.; Chen, Y.; Zhou, J. Synergetic photo-epoxidation of propylene with molecular oxygen over bimetallic Au–Ag/TS-1 photocatalysts. *Chinese J. Catal.* **2017**, *38*, 831–843. [[CrossRef](#)]
43. Hayden, P.; Sampson, R.J.; Spencer, C.B.; Pinnegar, H. Promoted Silver Catalyst for Producing Alkylene Oxides. Google Patents US4007135A, 8 February 1977.
44. Khatib, S.J.; Oyama, S.T. Direct oxidation of propylene to propylene oxide with molecular oxygen: A review. *Catal. Rev.* **2015**, 1–39. [[CrossRef](#)]
45. Carter, E.A.; Goddard, W.A. The surface atomic oxyradical mechanism for Ag-catalyzed olefin epoxidation. *J. Catal.* **1988**, *112*, 80–92. [[CrossRef](#)]
46. Amano, F.; Tanaka, T.; Funabiki, T. Steady-state photocatalytic epoxidation of propene by O₂ over V₂O₅/SiO₂ photocatalysts. *Langmuir* **2004**, *20*, 4236–4240. [[CrossRef](#)]
47. Oyama, S.T. Rates, kinetics, and mechanisms of epoxidation: homogeneous, heterogeneous, and biological routes. In *Mechanisms in Homogeneous and Heterogeneous Epoxidation Catalysis*; Oyama, S.T., Ed.; Elsevier: Amsterdam, The Netherlands, 2008; pp. 3–99. [[CrossRef](#)]
48. Taylor, B.; Lauterbach, J.; Delgass, W.N. Gas-phase epoxidation of propylene over small gold ensembles on TS-1. *Appl. Catal. A* **2005**, *291*, 188–198. [[CrossRef](#)]
49. Lu, J.; Zhang, X.; Bravo-Suárez, J.J.; Bando, K.K.; Fujitani, T.; Oyama, S.T. Direct propylene epoxidation over barium-promoted Au/Ti-TUD catalysts with H₂ and O₂: Effect of Au particle size. *J. Catal.* **2007**, *250*, 350–359. [[CrossRef](#)]
50. Liu, C.-H.; Guan, Y.; Hensen, E.J.M.; Lee, J.-F.; Yang, C.-M. Au/TiO₂@SBA-15 nanocomposites as catalysts for direct propylene epoxidation with O₂ and H₂ mixtures. *J. Catal.* **2011**, *282*, 94–102. [[CrossRef](#)]
51. Mizuno, N.; Yamaguchi, K.; Kamata, K. Epoxidation of olefins with hydrogen peroxide catalyzed by polyoxometalates. *Coord. Chem. Rev.* **2005**, *249*, 1944–1956. [[CrossRef](#)]
52. Farinas, E.T.; Alcalde, M.; Arnold, F. Alkene epoxidation catalyzed by cytochrome P450 BM-3 139-3. *Tetrahedron* **2004**, *60*, 525–528. [[CrossRef](#)]

